Analysis and performance of axial flux permanent magnet machine with air-cored non-overlapping concentrated stator windings (repository copy)

Analysis and Performance of Axial Flux Permanent-Magnet Machine With Air-Cored Nonoverlapping Concentrated Stator Windings

Maarten J. Kamper, *Member, IEEE*, Rong-Jie Wang, and Francois G. Rossouw

***Abstract*—In this paper, the performance of air-cored (ironless) stator axial flux permanent magnet machines with different types of concentrated-coil nonoverlapping windings is evaluated. The evaluation is based on theoretical analysis and is confirmed by finite-element analysis and measurements. It is shown that concentrated-coil winding machines can have a similar performance as that of normal overlapping winding machines using less copper.**

***Index Terms*—Air cored, axial flux, concentrated winding, permanent magnet (PM).**

NOMENCLATURE

a	Number of parallel circuits.
B_p	Peak air-gap flux density (in teslas).
e, E	Induced voltage (in volts).
h	Axial thickness of stator coil/winding (in meters).
k_p	Pitch factor.
k_d	Distribution factor.
k_e	End-winding factor.
k_f	Fill factor for stator conductors.
k_m	Winding mass factor.
k_r	Radius factor.
k_s	Stator factor.
k_w	Winding factor.
ℓ	Active length of stator coil/winding $= r_o - r_i$ (in meters).
ℓ_e	Total end-turn length of stator coil (in meters).
ℓ_g	Gap length between magnets of disks (in meters).
N	Number of coil turns.
n	Number of coils in a coil phase group.
$P_{\rm cu}$	Total copper losses of stator winding (in watts).
p	Number of poles.
Q	Number of stator coils.
q	Number of stator coils per phase $= Q/3$.
r_e	Average radius of stator winding $= (r_i + r_o)/2$ (in meters).
r_i	Inner radius of stator winding (in meters).
r_o	Outer radius of stator winding (in meters).
T_d	Developed torque (in newton meters).
w	Width of coil side (in meters).
λ	Flux linkage (in weber turns).
$\gamma_{\rm cu}$	Density of copper (in kilograms per cubic meter).
ρ_t	Resistivity of copper at temperature t (in ohmmeters).
θ_m	Defined coil pitch or coil span (in electrical radians).
θ_r	Coil width angle at radius r (in electrical radians).
ω	Electrical speed (in radians per second).

Paper IPCSD-07-119, presented at the 2007 IEEE International Electric Machines and Drives Conference, Antalya, Turkey, May 3–5, and approved for publication in the IEEE TRANSACTIONS ON INDUSTRY APPLICATIONS by the Electric Machines Committee of the IEEE Industry Applications Society. Manuscript submitted for review May 7, 2007 and released for publication January 21, 2008. Current version published September 19, 2008.

The authors are with the Department of Electrical and Electronic Engineering, University of Stellenbosch, Matieland 7602, South Africa.

I. INTRODUCTION

THE USE of concentrated nonoverlapping coils in radial flux permanent magnet (PM) electrical machines has certain advantages, among other things, 1) shorter overall axial length of the machine due to shorter end-turn length and 2) reduced stator winding cost due to less number of coils and simple winding structure. A drawback, in general, of concentrated-coil machines is the lower output torque due to a low winding factor. Recent studies, however, show that concentrated-coil PM machines with high pole numbers can have high winding factors and good output torque [1]–[4]. These studies focused on radial flux PM machines with iron-cored stators in the 5–150-Nm torque range. The characterization of an axial flux PM (AFPM) generator with an iron-cored concentrated winding is described in [5]. A research work on air-cored (ironless) concentrated-coil AFPM machines is reported in [6] and [7], but with no detailed analysis and comparison. Concentrated-coil AFPM machines with air-cored stators do not have the problem of cogging torque and putting the coils into iron slots as is the case with iron-cored stator machines. Hence, there is more freedom in the layout of the winding. Furthermore, concentrated-coil iron-cored PM machines are known for their additional core losses in the magnets and rotor iron yoke due to flux pulsations. In concentrated-coil air-cored AFPM machines, this is almost completely absent due to the low armature reaction effect. There are, thus, no disadvantages in using concentrated coils in air-cored stator AFPM machines, except for the remaining question on the torque performance when using these windings.

In this paper, the torque performance of concentrated-coil AFPM machines with air-cored stators is compared with the torque performance of those AFPM machines that use normal overlapping stator coil windings. The performance comparison is done by deriving analytical equations for the torque per given copper losses of the AFPM machines with different stator windings. As there are no iron losses in these machines and the eddy-current losses in the stator winding can be minimized by

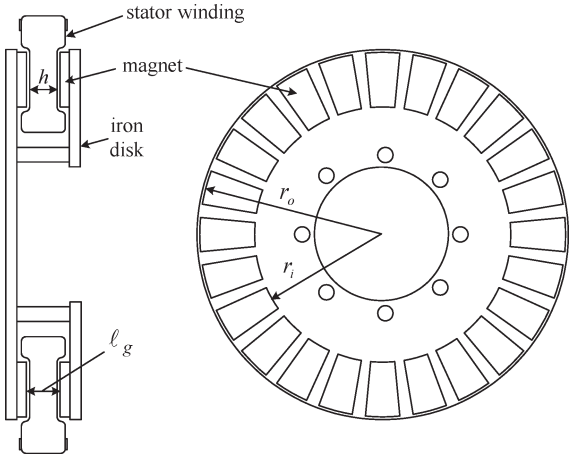

Fig. 1. Cross section of AFPM machine.

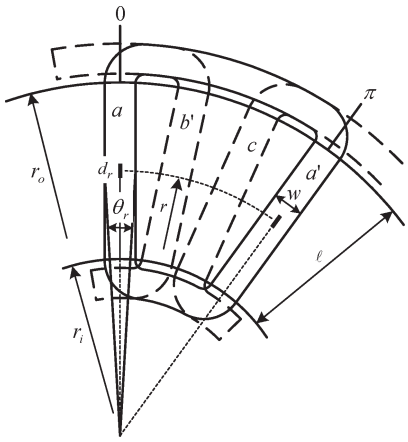

Fig. 2. Layout of normal overlapping stator winding.

using proper stator conductors [8]–[10], comparing the torque per copper losses of these machines is close to comparing the efficiency of the machines.

In Fig. 1, a drawing is shown of a typical AFPM machine with an air-cored stator. The stator shown is that of a normal overlapping stator winding with large end-winding overhang. Some dimensions are also shown.

II. Theoretical Analysis

In this section, analytical equations of the torque are derived for three-phase AFPM machines with three different stator windings, namely, the normal overlapping stator winding and two different types of concentrated-coil stator windings. Note that, in this analysis and in the performance comparison, only fundamental components of voltage and current are considered.

A. Normal Overlapping Stator Winding

The layout and dimensions of a normal three-phase overlapping air-cored stator winding are shown in Fig. 2. Only one coil per pole pair per phase is used in these types of windings; there is, in this case, no need for a distributed winding as a coil side is already distributed over one-third of a pole pitch, and furthermore, the axial air-gap flux density in these machines is

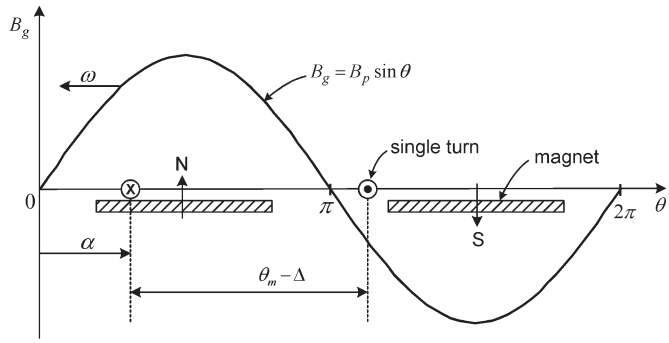

Fig. 3. Single-turn coil in sinusoidal field.

quite sinusoidal [7], [9]. From Fig. 3, assuming a sinusoidal axial flux density in the air gap, a coil pitch of $\theta_m = \pi$, and the coil at position α with respect to the flux density wave, the flux linkage of a turn element of radial length d_r at radius r can be determined by

$$\lambda = \int_{\alpha+\Delta}^{\alpha+\pi-\Delta} B_p \sin\theta_r d\theta \frac{2}{p} dr \tag{1}$$

with $-\theta_r/2 < \Delta < +\theta_r/2$. Executing the integral of (1) with $\alpha = \omega t$ results in the following for the element flux linkage:

$$\lambda = \left[\frac{4}{p} B_p r dr \cos(\Delta)\right] \cos(\omega t). \tag{2}$$

The element voltage $e_{\rm elm} = -d\lambda/dt$ is then given by

$$e_{\rm elm} = \left[\frac{4}{p} \omega B_p r dr \cos(\Delta)\right] \sin(\omega t). \tag{3}$$

Note that all the element voltages of (3) at the different Δ's are in phase as their magnetic axis are the same. From (3), the layer voltage, assuming a continuous layer with N conductors, can be determined by

$$e_{\rm layer} = \frac{4}{p} \omega B_p r dr N k_p \sin(\omega t) \tag{4}$$

with k_p given by

$$k_p = \frac{1}{\theta_r} \int_{\frac{-\theta_r}{2}}^{\frac{+\theta_r}{2}} \sin\left(\frac{\pi}{2} - \Delta\right) d\Delta$$

$$= \frac{2\sin(\theta_r/2)}{\theta_r}. \tag{5}$$

The coil voltage can be determined from (4) in a simple way by dividing the active length of the winding in a number of slices u, each with a length $dr_j = \ell/u$ at an average radius r_j as follows:

$$e_{\rm coil} = \frac{4}{p} \omega B_p N \left[\sum_{j=1}^{u} r_j \frac{\ell}{u} \frac{2\sin(\theta_{rj}/2)}{\theta_{rj}}\right] \sin(\omega t). \tag{6}$$

However, it was found that the term in brackets in (6) can be replaced with high accuracy by the term $r_e \ell k_p$, with k_p of (5) then defined as

$$k_p = \frac{2\sin(\theta_{re}/2)}{\theta_{re}}. \tag{7}$$

The peak value of the sinusoidal phase voltage E_p, therefore, can be written from (6) as

$$E_p = \frac{q}{a}\frac{4}{p}\omega B_p N r_e \ell k_p. \tag{8}$$

In the comparative study of the different windings, it is assumed that the phase current is in phase with the induced phase voltage. The developed torque of the machine, therefore, can be expressed from the developed power as

$$T_d = \frac{p}{2\omega}P_d = \frac{3p}{4\omega}E_p I_p \tag{9}$$

where I_p (i.e., the peak value of the sinusoidal phase current) can be expressed in terms of copper losses as

$$I_p = \sqrt{\frac{2P_{\rm cu}}{3R_{\rm ph}}} \tag{10}$$

and $R_{\rm ph}$ (i.e., the phase resistance) in turn as

$$R_{\rm ph} = \frac{N^2 q \rho_t (2\ell + \ell_e)}{a^2 k_f h w}. \tag{11}$$

The coil side width w can be expressed approximately as

$$w = 2r_e\theta_{re}/p. \tag{12}$$

Substituting (8), (10)–(12) in (9) leads to the following equation for the developed torque:

$$T_d = k_s k_e k_r C_1 \tag{13}$$

where k_s is a stator factor given by

$$k_s = k_p\sqrt{\theta_{re} q/p} \tag{14}$$

k_e is an end-winding factor given by

$$k_e = (2+\delta)^{-\frac{1}{2}}, \qquad \text{with } \delta = \ell_e/\ell \tag{15}$$

k_r is a radius factor given by

$$k_r = \sqrt{(1+\sigma_r)^3(1-\sigma_r)}, \qquad \text{with } \sigma_r = r_i/r_o \tag{16}$$

and C_1 is a machine constant at given copper losses given by

$$C_1 = r_o^2 B_p \sqrt{1.5 P_{\rm cu} k_f h/\rho_t}. \tag{17}$$

For normal overlapping air-cored windings, $Q = 3p/2$, so that $q/p = 1/2$ in (14). Furthermore, the inner radius where the coils are touching can be taken approximately as $r_i - \ell_g$. At this inner radius, the coil side width angle is $\pi/3$ electrical (note that the coil side width will always be a maximum to maximize k_s and the torque). As the coil side width w of (12) is a constant, it thus implies that $(r_i - \ell_g)\pi/3 = r_e\theta_{re}$. Hence, θ_{re} in (14) can be calculated by

$$\theta_{re} = \left(\frac{r_i - \ell_g}{r_e}\right)\frac{\pi}{3} = \frac{2\pi}{3}\left(\frac{\sigma_r - \xi}{1+\sigma_r}\right), \qquad \text{with } \xi = \ell_g/r_o. \tag{18}$$

TABLE I
STATOR AND END-WINDING FACTORS OF NORMAL OVERLAP WINDINGS

	$\sigma_r = 0.6$; $k_r = 1.28$					
	ξ=0.03			ξ=0.07		
p	k_s	k_e	$k_s k_e$	k_s	k_e	$k_s k_e$
14	0.597	0.494	0.295	0.577	0.472	0.272
16	0.597	0.508	0.303	0.577	0.484	0.279
20	0.597	0.530	0.316	0.577	0.503	0.290
24	0.597	0.547	0.326	0.577	0.517	0.298
28	0.597	0.559	0.334	0.577	0.527	0.304
32	0.597	0.569	0.340	0.577	0.536	0.309

An approximate formula for the average total end-turn length of practical overlapping coils is found to be

$$\ell_e = 4\pi r_e/p + 4\ell_g \tag{19}$$

so that δ in (15) can be expressed as

$$\delta = \frac{2\pi(1+\sigma_r)/p + 4\xi}{1-\sigma_r}. \tag{20}$$

Applying (12), the total mass of the copper of the stator winding is calculated by

$$M_{\rm cu} = k_m(2+\delta)C_2 \tag{21}$$

where k_m is a winding mass factor given by

$$k_m = \left(1-\sigma_r^2\right)\theta_{re} q/p \tag{22}$$

and C_2 is a machine constant given by

$$C_2 = 3r_o^2 k_f h \gamma_{\rm cu}. \tag{23}$$

From (13) and (21), it is clear that the torque and mass are expressed as functions of σ_r and ξ. The variable ξ depends on the outer diameter of the machine; extreme values for ξ are $0.01 < \xi < 0.1$. In the analysis, we used ξ as a parameter with typical values assigned to it, namely, $\xi = 0.03$ and $\xi = 0.07$. The ratio σ_r is varied in the analysis to investigate the change in torque and mass.

Some values for k_s and k_e are given in Table I with ξ as a parameter and $\sigma_r = 0.6$, and thus, $k_r = 1.28$ from (16); note that the latter values are typical values for overlap windings. As expected from the aforementioned equations, k_s is independent of the number of poles, whereas k_e and the overall winding factor and, hence, the torque of the machine improve with the number of poles. The effect of ξ on the overall winding factor is evident.

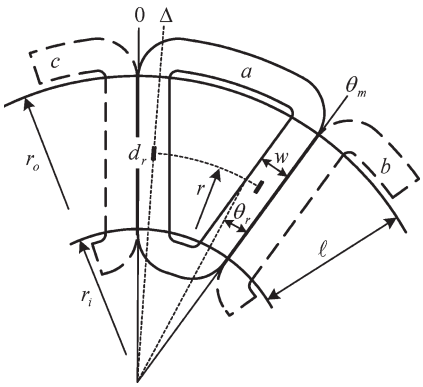

Fig. 4. Layout of concentrated nonoverlapping coil stator winding (type I).

B. Concentrated-Coil Stator Winding (Type I)

The layout and dimensions of a concentrated nonoverlapping air-cored stator winding are shown in Fig. 4. Only one coil in a phase band $(n = 1)$ is shown in this case, but more coils of the same phase $(n > 1)$ can be put side by side to form a coil phase group; thus, we have to look at the general case.

The procedure for the derivation of a torque equation for concentrated-coil windings is the same as for normal overlapping windings, except that θ_m, as shown in Fig. 4, is not a constant anymore but a variable that depends on the number of poles and number of stator coils as follows:

$$\theta_m = \pi p/Q. \tag{24}$$

Let $0 \le \Delta \le \theta_r$ in this case, and following the same procedure with the same approximations as in Section II-A, a similar equation for the peak value of the phase voltage as in (8) can be determined as

$$E_{\rm pc} = \frac{q}{a}\frac{4}{p}\omega B_p N r_e \ell k_{p(I)} k_{d(I)} \tag{25}$$

where the pitch factor $k_{p(I)}$ in this case is

$$k_{p(I)} = \frac{\sin\left[0.5\theta_m(1-\kappa)\right]\sin(0.5\kappa\theta_m)}{0.5\kappa\theta_m}, \qquad \text{with } \kappa = \frac{\theta_{re}}{\theta_m} \tag{26}$$

and $k_{d(I)}$ is a distribution factor that takes into account the effect on the induced phase voltage when two or more coils are connected in series in a coil phase group $(n > 1)$

$$k_{d(I)} = \frac{\sin\left[0.5n(\theta_m - \pi)\right]}{n\sin\left[0.5(\theta_m - \pi)\right]}. \tag{27}$$

Note that (27) gives the distribution factor of those coil phase groups of which the n coils are side by side together, and not of unevenly distributed coils in a phase group.

The aforementioned analysis is actually more complex than in (25)–(27) because 1) the actual average length of the active part of the winding is slightly larger than ℓ and 2) the active part is slightly skewed with the radial flux distribution as can be seen from Fig. 4. These effects, however, become negligible when the pole number is high.

Following the same procedure for the developed torque as in (13), the following torque equation is obtained for concentrated-coil winding machines:

$$T_{dc} = k_{sc} k_{ec} k_r C_1. \tag{28}$$

In (28), the stator factor k_{sc} is given by

$$k_{sc} = k_{wc}\sqrt{\kappa\pi/3}, \qquad \text{with } k_{wc} = k_{p(I)}k_{d(I)} \tag{29}$$

where k_{wc} is the winding factor equivalent to the general winding factor of electrical machines. κ in (29) is not a constant but must be $\kappa \le \kappa(\max)$, where $\kappa_{(\max)}$ is shown in Fig. 4 as

$$\kappa_{(\max)} = \frac{\theta_{re(\max)}}{\theta_m} = \frac{r_i}{2r_e} = \frac{\sigma_r}{1+\sigma_r}. \tag{30}$$

The end-winding factor k_{ec} in (28) is given by

$$k_{ec} = (2+\delta_c)^{-\frac{1}{2}}, \qquad \text{with } \delta_c = \ell_{ec}/\ell \tag{31}$$

and ℓ_{ec} is the average total end-turn length of a concentrated coil. The accurate calculation of ℓ_{ec} [and ℓ_e in (19)] is very important as it largely affects the comparison results; a formula to calculate ℓ_{ec} for practical concentrated coils is found to be

$$\ell_{ec} = 2\theta_m(r_o + r_i)(1 - 0.6\kappa)/p. \tag{32}$$

From (31) and (32), δ_c can thus be expressed as

$$\delta_c = \frac{2\theta_m}{p}\left(\frac{1+\sigma_r}{1-\sigma_r}\right)(1 - 0.6\kappa). \tag{33}$$

As in (21), the total mass of the copper of the concentrated-coil winding is calculated by

$$M_{\rm cu(c)} = k_m(2+\delta_c)C_2. \tag{34}$$

Various layouts exist for concentrated-coil windings. The procedure to determine valid layouts for three-phase concentrated-coil windings is as follows:

1) Select the number of poles divisible by two.
2) Identify those i's, where i is a positive integer that meet the following:

$$36 \cdot \left[\frac{p}{6i} - \text{TRUNC}\left(\frac{p}{6i}\right)\right] = k, \qquad k = 6, 12, 24, \text{ or } 30.$$

3) For $n = 1, 2, \ldots$ (i.e., the number of phase coils side by side forming a coil phase group), calculate the possible number of stator coils as $Q = 3ni$.

It is interesting to investigate the stator winding factors k_{wc}, k_{sc}, and k_{ec} as functions of κ. As an example, we choose a 32-pole AFPM machine with two possible stator windings, namely, with $Q = 24$ $(n = 1)$ and $Q = 30$ $(n = 5)$ and, furthermore, with $\sigma_r = 0.6$. The results of the calculations are shown in Figs. 5 and 6. An interesting result is that the winding factor k_{wc} of the $p = 32$ $Q = 24$ stator winding can be higher than that of the $p = 32$ $Q = 32$ winding. More important,

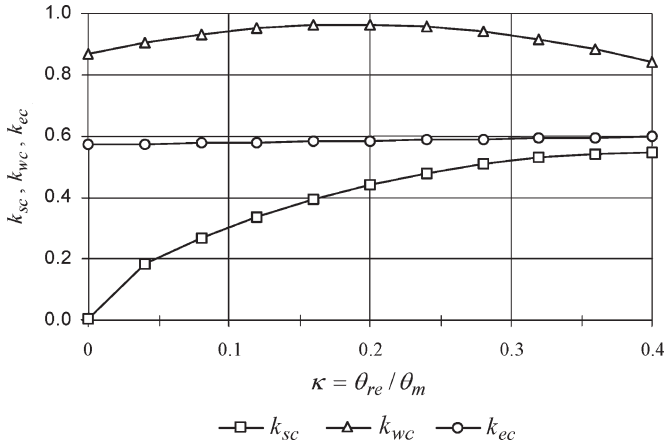

Fig. 5. Stator winding factors of $p = 32$ $Q = 24$ $n = 1$ AFPM machine ($\sigma_r = 0.6$) (type I).

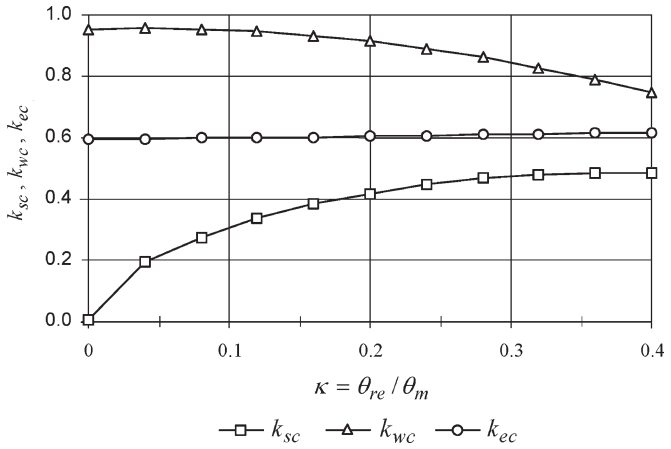

Fig. 6. Stator winding factors of $p = 32$ $Q = 30$ $n = 5$ AFPM machine ($\sigma_r = 0.6$) (type I).

however, is the stator factor k_{sc} that directly affects the torque of the AFPM machine according to (28); the highest torque is obtained with $\kappa = \kappa_{(\max)} = 0.375$ from (30). Note importantly that the highest torque is not obtained where the general electrical machine winding factor k_{wc} is the highest. The end-winding factor k_{ec} is shown to be hardly affected by κ.

To choose the layout with the highest output torque, it is best to select the layout with the highest factor $k_{sc}k_{ec}$. In Table II, the best options for concentrated-coil windings are given for a different number of poles. In each case, κ was optimized to maximize $k_{sc}k_{ec}$, keeping $\kappa \leq \kappa_{(\max)}$; however, it was found that, in all the cases, $\kappa_{(\text{optimum})} \approx \kappa_{(\max)}$.

From these results, it is clear that the best options are those windings where the number of poles are divisible by four and $n = 1$; this results in winding layouts with $\theta_m = 4\pi/3$ (240° electrical), a significant result that makes the design of AFPM machines with concentrated-coil windings very simple. Note that this finding still holds when other more complex unevenly distributed winding layouts are also considered. Furthermore, from the results in Table II, it can be seen that the end-winding factor k_{ec} improves with Q, as expected, and $k_{sc}k_{ec}$ improves with pole number; note that k_{sc} is independent of pole number for the best winding options.

TABLE II
STATOR WINDING FACTORS OF CONCENTRATED-COIL (TYPE I) WINDINGS

$\sigma_r = 0.6$; $k_r = 1.28$					
p	n	Q	k_{sc}	k_{ec}	$k_{sc}k_{ec}$
14	2	12	0.509	0.525	0.267
	4	12	0.441	0.525	0.232
	5	15	0.452	0.551	0.249
16	1	12	**0.545**	0.525	**0.286**
	2	12	0.472	0.525	0.248
	5	15	0.486	0.551	0.267
18	1	27	0.372	0.606	0.225
20	1	12	**0.530**	0.525	0.278
	1	15	**0.545**	0.551	**0.300**
	3	18	0.496	0.570	0.283
22	3	18	0.452	0.570	0.257
	4	24	0.448	0.596	0.267
	7	21	0.481	0.585	0.281
24	1	18	**0.545**	0.570	**0.310**
	2	18	0.472	0.570	0.269
	3	27	0.440	0.606	0.267
26	4	24	0.490	0.596	0.292
	8	24	0.424	0.596	0.253
	9	27	0.460	0.606	0.279
28	1	21	**0.545**	0.585	**0.319**
	2	24	0.509	0.596	0.304
	9	27	0.479	0.606	0.290
30	1	18	0.530	0.570	0.302
	2	36	0.424	0.627	0.266
	3	27	0.496	0.606	0.301
32	1	24	**0.545**	0.596	**0.325**
	2	24	0.472	0.596	0.282
	5	30	0.486	0.614	0.298

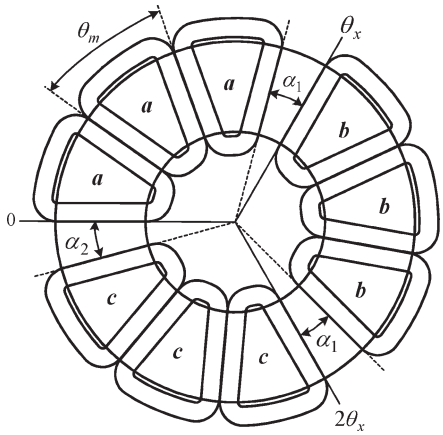

Fig. 7. Layout of phase-group concentrated-coil stator winding ($n = 3$).

C. Phase-Group Concentrated-Coil Stator Windings

Phase-group concentrated-coil stator windings are defined as those windings where $n = q = Q/3$; this implies that all the coils of a coil phase group are grouped together in space on one-third of the circumference of the machine as shown in Fig. 7. Examples of these stator windings with fairly good winding factors are given in Table II, e.g., $\{p = 16, Q = 15\}$, $\{p = 22, Q = 21\}$, and $\{p = 28, Q = 27\}$. Note that, with these air-cored phase-group windings, there is no disadvantage of unbalanced magnetic pull or an increase in magnetic noise, as is the case with iron-cored concentrated-coil stators [4].

TABLE III
STATOR WINDING FACTORS OF PHASE-GROUP CONCENTRATED WINDINGS

$\sigma_r = 0.6;\quad k_r = 1.28$								
p	n	Q	$\alpha_1°$	$\alpha_2°$	k_θ	$k_{sc(ph)}$	$k_{ec(ph)}$	$k_{sc}k_{ec(ph)}$
14	4	12	11.4	11.4	0.905	0.471	0.537	0.253
16	5	15	3.24	3.24	0.973	**0.487**	0.554	**0.27**
18	5	15	9.29	29.3	0.918	0.460	0.566	0.260
20	6	18	9.00	9.00	0.925	0.474	0.577	0.274
22	7	21	3.24	3.24	0.973	**0.486**	0.587	**0.285**
24	7	21	8.05	23.1	0.930	0.465	0.595	0.277
26	8	24	7.44	7.44	0.938	0.477	0.602	0.287
28	9	27	2.76	2.76	0.977	**0.486**	0.608	**0.296**
30	9	27	6.61	18.6	0.943	0.47	0.613	0.288
32	10	30	6.24	6.24	0.948	0.479	0.618	0.296

Referring to Fig. 7, the highest winding factor for phase-group concentrated-coil stator windings for any pole number can be obtained by using the following θ_m in (26), (27), and (33):

1) For pole numbers divisible by three ($p = 6, 12, 18, \ldots$)

$$\theta_x = 2\pi/3 \pm 1/p \qquad Q = p - 3 \qquad n = Q/3$$

$$\theta_m = k_\theta \left(\frac{3p}{Q}\right)(\pi - \theta_x), \qquad \text{for } \theta_x > 2\pi/3$$

$$\theta_m = k_\theta \left(\frac{3p}{2Q}\right)\theta_x, \qquad \text{for } \theta_x < 2\pi/3.$$

2) For pole numbers not divisible by three (e.g., $p = 14, 16, 20, \ldots$)

$$Q = 3n = 3 \cdot \text{ROUND}(p/3 - 0.5)$$

$$\theta_m = k_\theta \frac{\pi p}{Q} \qquad \theta_x = 2\pi/3$$

with k_θ as a real value (typical: $0.9 \le k_\theta \le 1$) to be optimized to maximize the winding factor; note that θ_x is a mechanical angle.

For the calculation of the winding factors, the torque and the mass of copper for phase-group windings, the same equations as in Section II-B, are used. The results of the highest winding factors for phase-group windings are given in Table III; note that, in each case, κ was optimized to maximize $k_{sc}k_{ec}$, and in each case, $\kappa \le \kappa_{(\max)}$ according to (30). It can be seen that machines with pole numbers not divisible by three give slightly better winding factor values; these values are also slightly higher than the values given in Table II as $k_\theta < 1$ in this case.

D. Concentrated-Coil Winding (Type II)

A second-type concentrated-coil winding shown in Fig. 8 was investigated; the difference with the first type (Fig. 4) is that the coils are touching each other only at the inner radius.

It is clear that this layout will lead to less flux linkage, but the advantage is that the end-turn length is shorter. The derivation

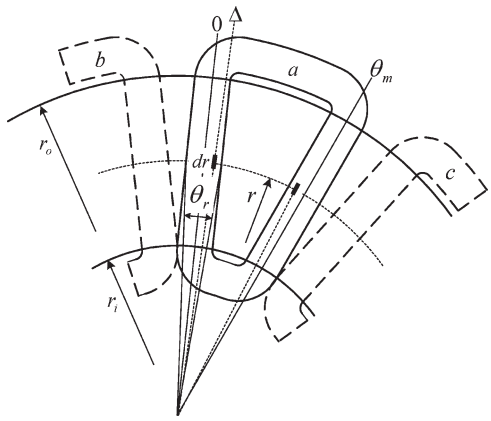

Fig. 8. Layout of concentrated-coil (type II) stator winding.

of the stator factor $k_{sc(\text{II})}$ is the same as in (26), (27), and (29), however, with a different result, namely,

$$k_{sc(\text{II})} = k_{wc(\text{II})}\sqrt{\theta_{re}q/p}, \qquad \text{with } k_{wc(\text{II})} = k_{p(\text{II})}k_{d(\text{II})} \tag{35}$$

with the pitch factor given by

$$k_{p(\text{II})} = \frac{\sin(\theta_m/2)\sin(\theta_{re}/2)}{\theta_{re}/2} \tag{36}$$

and the distribution factor by

$$k_{d(\text{II})} = \frac{\sin\left[0.5n(\theta_i - \pi)\right]}{n\sin\left[0.5(\theta_i - \pi)\right]} \tag{37}$$

where $\theta_i = \pi p/Q$ and θ_m is given by

$$\theta_m = \theta_i - 0.5\theta_{re}(1 + 1/\sigma_r). \tag{38}$$

The equation for the average total end-turn length of the type II concentrated-coil winding is

$$\ell_{ec(\text{II})} = 2(r_o + r_i)[\theta_m + 0.4\theta_{re}]/p \tag{39}$$

so that δ_c of (33) can be expressed for the type II winding as

$$\delta_{c(\text{II})} = \frac{2}{p}\left(\frac{1+\sigma_r}{1-\sigma_r}\right)(\theta_m + 0.4\theta_{re}). \tag{40}$$

θ_{re} must be optimized to maximize $k_{sc(\text{II})}$ of (35), however, with the restriction that

$$\theta_{re} \le \theta_{re(\max)} = \left(\frac{\sigma_r}{1+\sigma_r}\right)\theta_i. \tag{41}$$

For the calculation of the torque and the mass of copper using this type of winding, (28) and (34) of Section II-B are used. Some results of the winding factors for the type II concentrated winding are given in Table IV. As with the type I concentrated winding, the highest values for the winding factors are obtained for pole numbers divisible by four and $n = 1$.

TABLE IV
STATOR WINDING FACTORS OF CONCENTRATED-COIL TYPE II WINDING

$\sigma_r = 0.6$; $k_r = 1.28$					
p	n	Q	$k_{sc(II)}$	$k_{ec(II)}$	$k_{sc(II)}k_{ec(II)}$
16	1	12	**0.5**	0.54	**0.269**
	2	12	0.432	0.54	0.233
28	1	21	**0.5**	0.595	**0.297**

TABLE V
WINDING DATA AND TORQUE PERFORMANCE COMPARISON

$\sigma_r = 0.6$; $k_r = 1.28$							
Winding type	p	n	Q	k_s	k_e	$k_s k_e$	T_d (pu)
Overlap ξ=0.03	16	1	24	0.597	0.508	0.303	0.95
Overlap ξ=0.07	16	1	24	0.577	0.484	0.279	0.87
Concentrated I	16	1	12	0.545	0.525	0.286	0.90
Phase-group	16	5	15	0.487	0.554	0.27	0.85
Concentrated II	16	1	12	0.5	0.54	0.269	0.84
Overlap ξ=0.03	28	1	42	0.597	0.559	0.334	1.05
Overlap ξ=0.07	28	1	42	0.577	0.527	0.304	0.95
Concentrated I (**base**)	28	1	21	0.545	0.585	0.319	1.0
Phase-group	28	9	27	0.486	0.608	0.296	0.93
Concentrated II	28	1	21	0.5	0.595	0.297	0.93

E. Torque and Copper Mass Comparison

The comparison study is done on a per unit basis. It is therefore not necessary to calculate the machine constants C_1 and C_2 of (17) and (23), but only the overall winding factor $k_s k_e k_r$ and mass factor $k_m(2+\delta)$. Table V summarizes the results of Tables I–IV for windings with pole numbers $p = 16$ and $p = 28$; windings with these pole numbers have the best winding factors for all three types of concentrated windings. The comparison in Table V is with $\sigma_r = 0.6$, but Figs. 9 and 10 show the effect of the σ_r ratio on the torque generated by the different windings. Note that, in Table V and Figs. 9 and 10, the torque (actually $k_s k_e k_r$) of the $p = 28$ AFPM machine with the type I concentrated-coil winding (Fig. 4) is taken as the base value for the per unit torque calculations.

From Table V, it can be seen that the end-winding factor plays an important role in the torque performance. Table V and Figs. 9 and 10 show also that the end-winding parameter ξ (between $\xi = 0.03$ and $\xi = 0.07$) has a substantial effect (8%–9%) on the developed torque of the overlapping winding; note that $\xi = 0.07$ is more typical than $\xi = 0.03$. From the comparison results, it is clear that the type I concentrated-coil winding is the best of the three types of nonoverlapping windings considered; the torque performance of this winding compares also favorably with that of the overlapping winding.

Further observations are the following: 1) the optimum σ_r values for the windings are different and 2) the performance of the nonoverlapping concentrated windings with respect to the overlapping winding improves with pole number as δ_c reduces; nonoverlapping concentrated windings are, thus, best suited for high-pole-number AFPM machines.

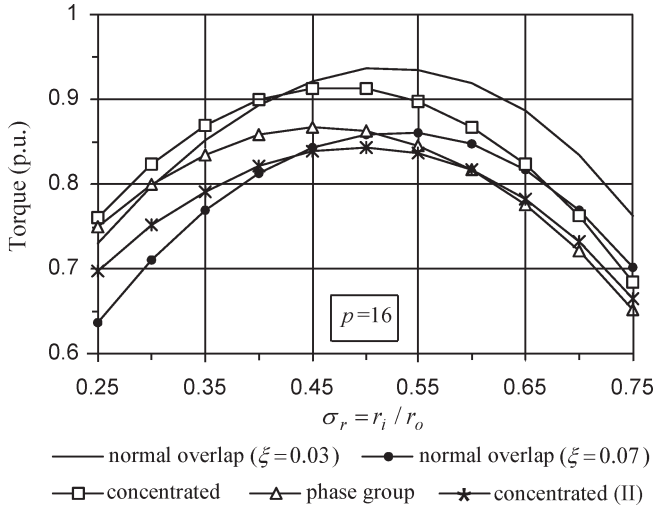

Fig. 9. Per-unit torque versus σ_r for different stator windings of $p = 16$ AFPM machine.

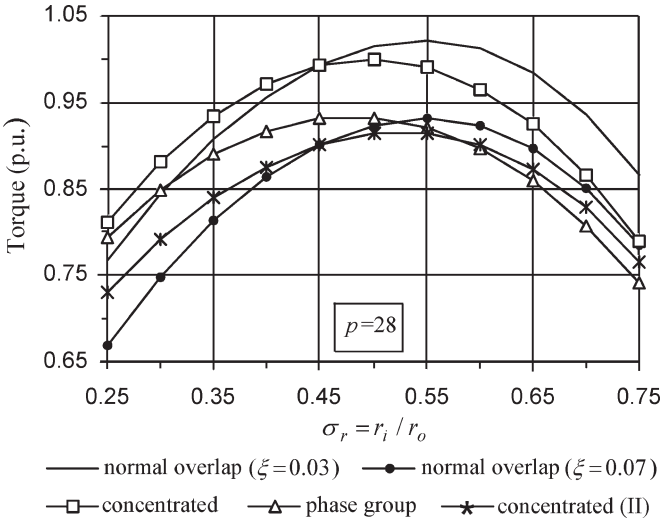

Fig. 10. Per-unit torque versus σ_r for different stator windings of $p = 28$ AFPM machine.

In Figs. 11 and 12, the effect of the σ_r ratio on the per unit mass of the copper of the different windings is shown; note that at one per unit torque, the mass of the copper [actually $k_m(2+\delta)$] of the $p = 28$ type I concentrated-coil winding is taken as the base value for the per unit mass calculations. The low copper mass and good torque per copper mass of specifically the concentrated type II winding are noteworthy from Figs. 9–12.

It is also clear that higher pole number machines use less copper than low-pole-number machines.

Finally, it is interesting from Figs. 11 and 12 that the copper mass and thus copper cost increase with an increase in σ_r (except at high σ_r ratios); this is due to an increase in coil width as more space become available for coils at the inner radius. In contrast, however, magnet mass and cost vary with $(1-\sigma_r^2)$, so that magnet cost decreases with an increase in σ_r. Magnet mass and cost, therefore, must also be considered in a complete comparison.

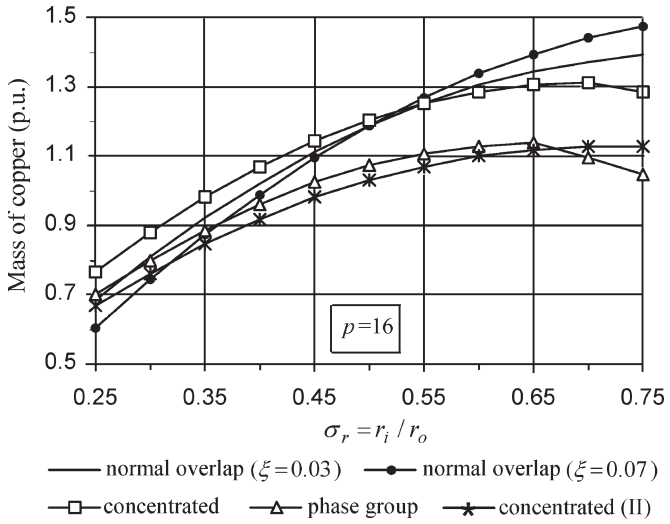

Fig. 11. Per unit mass of copper versus σ_r for different stator windings of $p = 16$ AFPM machine.

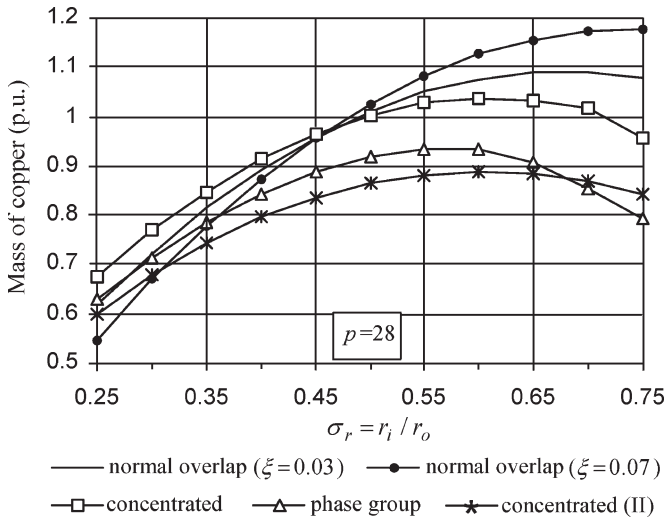

Fig. 12. Per unit mass of copper versus σ_r for different stator windings of $p = 28$ AFPM machine.

III. Numeric Modeling and Measurements

To evaluate the performance capability of the AFPM machine with different winding topologies, three air-cored AFPM stators, with normal overlapping type I concentrated-coil and phase-group windings, have been designed and fabricated as shown in Fig. 13. These stators have been designed for the same PM rotor disks. The complete design data of the AFPM machines are given in Table VI.

Fig. 14 shows 2-D finite-element (FE) models of the normal three-phase overlapping winding and two types of concentrated-coil AFPM machines. Owing to the axial symmetry, it is only necessary to model half of the machine for all three types of AFPM machines, i.e., one rotor disk and half a stator, by applying Neumann condition on the top boundary.

For a normal overlapping winding AFPM machine [Fig. 14(a)], it is possible to model just one pole pitch of the machine by applying negative periodical conditions on the left and right boundaries. However, for type I concentrated winding AFPM machines [Fig. 14(b)], it is necessary to model two pole pairs of the machine by using positive periodical conditions. For the phase-group winding AFPM machine [Fig. 14(c)], it is inevitable to model the complete machine as there is no symmetry in the coil groups.

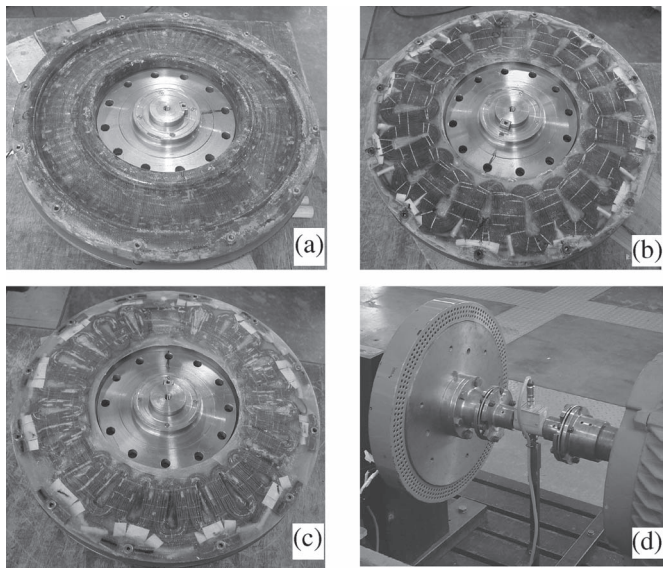

Fig. 13. Air-cored AFPM machine stators with (a) normal overlapping winding, (b) concentrated winding, (c) phase-group winding, and (d) the testing setup of the AFPM machine.

TABLE VI
Design Data of AFPM Machines With Different Winding Topologies

Design data	overlap	non-overlap	phase-group
Output power (kW)	1	1	1
Speed (r/min)	200	200	200
Number of phases	3 (wye)	3 (wye)	3 (wye)
Rated line voltage (V)	19.9	19.6	18.4
Frequency (Hz)	40	40	40
Number of poles	24	24	24
Number of stator coils	36	18	21
Number of turns per coil	11	25	23
Wire diameter (mm)	0.8	0.85	0.7
Number of parallel wires	7	6	6
Axial height of PM (mm)	6	6	6
Winding axial thickness (mm)	8.4	8.4	8.4
Air-gap (one side) (mm)	1.8	1.8	1.8
Air gap flux density (T)	0.527	0.527	0.527
Outer PM diameter (mm)	400	400	400
$\sigma_r = r_{in}/r_{out}$ ratio	0.7	0.7	0.7
Cooling	air-cooled	air-cooled	air-cooled

A. Measured Results

The small (1 kW) AFPM machine shown in Fig. 13(d) was tested as a generator feeding a balanced three-phase resistive load. An ac drive was used as prime mover and a torque transducer to measure the shaft torque as shown in Fig. 13(d).

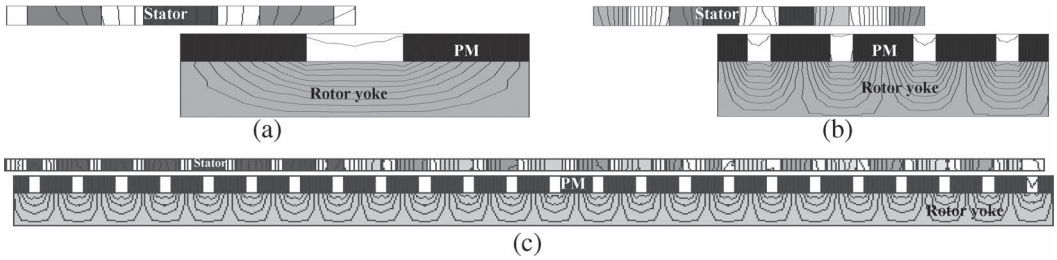

Fig. 14. 2-D FE models of air-cored AFPM generator with (a) normal overlapping, (b) concentrated winding, and (c) phase-group winding.

TABLE VII
COMPARISON OF CALCULATED AND MEASURED RESULTS

	P_{cu}=120 W; ξ=0.06; k_r = 1.214; r_o = 200 mm								
	n	Q	$k_s k_e$	$T_{d(calc)}$	$T_{d(FEA)}$	$T_{d(neas)}$	$k_m(2+\delta)$	$M_{Cu(calc)}$	$M_{Cu(meas)}$
Overlap	-	36	0.296	45.87	44.36	43.9	0.861	3.245	3.484
Concentrated	1	18	0.292	45.31	45.13	44.6	0.767	2.891	2.977
Phase-group	7	21	0.262	40.59	39.54	39.7	0.589	2.217	2.175

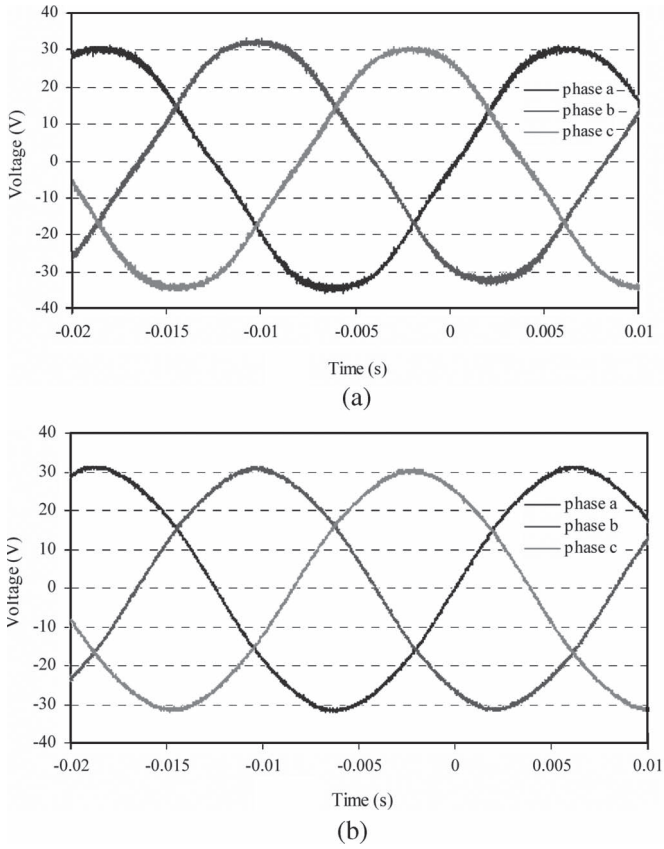

Fig. 15. Measured open circuit voltage waveform of AFPM machine with (a) overlapping and (b) concentrated winding.

The machine was tested at the same copper loss of 120 W for each type of stator winding used.

The machine data and calculated and measured results are given in Table VII. The good agreement between the calculations and measurements in the torque and copper-mass comparisons of the three windings is evident. Fig. 15 shows the measured induced open circuit voltage of the normal overlap and the type I concentrated windings. It is clear that an improved sinusoidal voltage waveform is obtained with the concentrated winding.

IV. CONCLUSION

The analysis and measured results show that AFPM machines with air-cored nonoverlap concentrated-coil windings can have similar and, in some cases, better torque performance than with normal overlap windings; also, the higher the pole number, the more competitive the concentrated winding becomes. From the derived winding factors, the best pole–coil combinations for the different concentrated windings are identified. A significant result for concentrated windings with one coil per phase group is that a coil span of 240° electrical and pole numbers divisible by four can be used throughout. It is furthermore shown that the mass of copper used is less with concentrated windings—the test machine, for example, uses almost 15% less copper with the concentrated winding than with the overlapping winding. The concentrated winding also shows the generation of a much more sinusoidal induced voltage waveform than the overlap winding.

REFERENCES

[1] J. Cros and P. Viarouge, "Synthesis of high performance PM motors with concentrated windings," *IEEE Trans. Energy Convers.*, vol. 17, no. 2, pp. 248–253, Jun. 2002.

[2] F. Magnussen and C. Sadarangani, "Winding factors and joule losses of permanent magnet machines with concentrated windings," in *Proc. IEEE IEMDC*, Madison, WI, Jun. 2003, pp. 333–339.

[3] F. Magnussen, P. Thelin, and C. Sadarangani, "Performance evaluation of permanent magnet synchronous machines with concentrated and distributed windings including the effect of field-weakening," in *Proc. IEE Int. Conf. Power Electron., Mach. Drives*, Edinburgh, U.K., Mar./Apr. 2004, pp. 679–685.

[4] F. Libert and J. Soulard, "Investigation on pole-slot combinations for permanent-magnet machines with concentrated windings," in *Proc. ICEM*, Sep. 2004, p. 530.

[5] G. Tomassi, M. Topor, F. Marignetti, and I. Boldea, "Characterization of an axial-flux machine with non-overlapping windings as a generator," *Electromotion*, vol. 13, no. 1, pp. 73–79, Jan.–Mar. 2006.

[6] A. Parviainen, J. Pyrhonen, and P. Kontkanen, "Axial flux permanent magnet generator with concentrated winding for small wind power applications," in *Proc. IEEE Int. Conf. Elect. Mach. Drives*, May 15, 2005, pp. 1187–1191.

[7] J. R. Bumby and R. Martin, "Axial-flux permanent-magnet air-cored generator for small-scale wind turbines," *Proc. Inst. Electr. Eng.—Electr. Power Appl.*, vol. 152, no. 5, pp. 1065–1075, Sep. 2005.

[8] R.-J. Wang and M. J. Kamper, "Calculation of eddy current loss in axial field permanent-magnet machine with coreless stator," *IEEE Trans. Energy Convers.*, vol. 19, no. 3, pp. 532–538, Sep. 2004.

[9] J. F. Gieras, R.-J. Wang, and M. J. Kamper, *Axial Flux Permanent Magnet Brushless Machines*. Dordrecht, The Netherlands: Kluwer, 2004.

[10] R.-J. Wang, M. J. Kamper, K. Van der Westhuizen, and J. F. Gieras, "Optimal design of a coreless stator axial flux permanent-magnet generator," *IEEE Trans. Magn.*, vol. 41, no. 1, pp. 55–64, Jan. 2005.